Journal of Surgery
Fujiwara H, et al. J Surg 8: 1759
www.doi.org/10.29011/2575-9760.001759
www.gavinpublishers.com

OPEN ACCESS

GAVIN PUBLISHERS

Case Report

A Case of Laparoscopically Resected Rectal Neuroendocrine Carcinoma and Its Renal Metastasis with a Potential Sensitivity to Inhibitors of FGFR and the Bcl Family

Hajime Fujiwara[1#], Satoshi Nagayama[1,2#*], Hiroshi Kawachi[3], Kaoru Nakano[3], Yuki Shimizu[4], Ryohei Katayama[4], Ryoji Yao[5], Yoshinobu Komai[6], Yukiharu Hiyoshi[1], Toshiki Mukai[1], Tomohiro Yamaguchi[1], Toshiya Nagasaki[1], Takashi Akiyoshi[1], Yosuke Fukunaga[1]

[1]Department of Colorectal Surgery, Gastroenterological Cancer Center, Cancer Institute Hospital, Japanese Foundation for Cancer Research, Tokyo, Japan

[2]Department of Surgery, Uji-Tokusyukai Medical Center, Kyoto, Japan

[3]Department of Pathology, Cancer Institute Hospital, Japanese Foundation for Cancer Research, Tokyo, Japan

[4]Division of Experimental Chemotherapy, Cancer Chemotherapy Center, Japanese Foundation for Cancer Research, Tokyo, Japan

[5]Department of Cell Biology, The Cancer Institute, Japanese Foundation for Cancer Research, Tokyo, Japan

[6]Department of Genitourinary Oncology, Cancer Institute Hospital, Japanese Foundation for Cancer Research, Tokyo, Japan

[#] These authors contributed equally to this work.

[*]**Corresponding author:** Satoshi Nagayama, Department of Surgery, Uji-Tokusyukai Medical Center, 145 Makishima-cho Ishibashi, Uji, Kyoto, 611-0041, Japan

Citation: Fujiwara H, Nagayama S, Kawachi H, Kaoru N, Shimizu Y, Katayama R, et al. (2023) A Case of Laparoscopically Resected Rectal Neuroendocrine Carcinoma and Its Renal Metastasis with a Potential Sensitivity to Inhibitors of FGFR and the Bcl Family. J Surg 8: 1759 DOI: 10.29011/2575-9760.001759

Received Date: 17 March, 2023; **Accepted Date:** 27 March, 2023; **Published Date:** 29 March, 2023

Abstract

We present an extremely rare case of rectal neuroendocrine carcinoma with solitary renal metastasis. A 56-year-old woman presented with melena and subsequent colonoscopy revealed a rectal tumor which was diagnosed as neuroendocrine carcinoma by tumor biopsy. Furthermore, a solitary 14x10mm renal metastasis was highly suspected by CT, MRI, PET and octreotide scintigraphy. Upon completion of four courses of systemic chemotherapy with CDDP+CPT11, both the primary and metastatic lesions were stable and there was no evidence of new metastatic lesions. Thus, we performed a radical operation by laparoscopic low anterior resection along with a partial nephrectomy. Pathological examination confirmed the renal tumor to be a metastatic lesion from the rectal neuroendocrine carcinoma. The patient is currently being monitored carefully without any adjuvant chemotherapy. At two years after the operation, there is no evidence of local recurrence or distant metastasis. Whole exome sequencing of the primary and metastatic tumors showed common mutations including APC, RB1 and TP53. There were no significantly different mutations detected between the primary and metastatic lesions, suggesting a low possibility of the involvement of any specific mutations to drive renal metastasis. In addition, through our comprehensive drug sensitivity screening system of 92 inhibitors using the patient-derived cell lines (PDCs), both FGFR inhibitor (infigratinib) and Bcl family inhibitors (obatoclax and navitoclax) were found to have a significant antiproliferative effect in the PDCs established from the primary lesion.

Mini-Abstract

An extremely rare case of rectal neuroendocrine carcinoma with solitary renal metastasis was successfully treated by intensive systemic chemotherapy and subsequent laparoscopic radical resection of the primary and metastatic lesions.

Keywords: Drug sensitivity screening; Renal metastasis; Rectal neuroendocrine carcinoma; Whole exome sequencing

Introduction

According to the new World Health Organization (WHO) classification of Gastroenteropancreatic Neuroendocrine Neoplasia (GEP-NEN), [1] Neuroendocrine Carcinoma (NEC) is defined as a distinct disease entity different from neuroendocrine tumor (NET) that constitutes well-differentiated NEN. Specifically, NEC is characterized by poor differentiation, mitotic rates greater than 20 mitoses per $2mm^2$ and a Ki-67 index higher than 20%. While the origin of GEP-NEC remains elusive, [2] the existence of mixed neuroendocrine-non-neuroendocrine neoplasms (MiNEN) suggests that GEP-NEN and non-NEN components develop from a common precursor lesion. [3] A comprehensive molecular characterization by whole-genome sequencing has revealed frequent genetic alterations in TP53 and RB1 in GEP-NECs. [2,4,5] Because of the scarcity of patients with NEC, there are no standard treatment flowcharts established. Since NECs are invariably aggressive and frequently metastasize to distant organs, resulting in an extremely poor prognosis, the first-choice treatment is considered to be intense systemic chemotherapy even if radical resection seems feasible. The clinical benefit of the resection of primary colorectal and metastatic lesions for macroscopic eradication of cancer cells has yet to be determined, so the actual management of well-advanced NECs depends on the decisions arrived at through multidisciplinary discussions in each case. Here, we present an extremely rare case of a rectal NEC with a solitary renal metastasis which were macroscopically resected by a laparoscopic approach following intensive systemic chemotherapy with CDDP and CPT11.

Case Presentation

A 56-year-old woman was referred to our hospital for further examination of melena. There were no significant abnormalities including tumor markers (CEA: 1.4ng/ml, CA15-3: 2.0U/ml). Upon rectal examination, a tethered tumor was felt on the anterior wall of the rectum, 8 cm above the anal verge. Subsequent colonoscopy revealed a type 2 tumor at the upper rectum, and pathological examination of biopsied samples from it showed an infiltrative proliferation of carcinoma cells characterized by a high nuclear-cytoplasmic (N/C) ratio and prominent nucleoli. Immunohistochemical staining was positive for both synaptophysin and chromogranin A, and the Ki-67 index was higher than 90% (Figure 1). These pathological findings confirmed by two experienced pathologists (HK and KN) led to a definitive diagnosis of rectal NEC. Contrast-enhanced Computed Tomographic (CT) scans revealed a tumor of 30 mm in size on the anterior-left wall of the rectum, which was suspected to infiltrate through the rectal wall. Although no significantly swollen lymph nodes were detected, an enhanced mass lesion of 15 mm in size was observed at the upper pole of the right kidney (Figure 2). On renal magnetic resonance (MR) imaging, the tumor was isointense and hyperintense compared to renal parenchyma on T1- and T2-weighted images, respectively. In addition, the mass lesion was hyperintense on diffusion-weighted images and clearly enhanced with contrast material (Figure 2). Positron emission tomography with 18-Fluorodeoxyglucose (FDG-PET) showed increased uptake signals in the mass lesions on the anterior-left rectal wall (SUVmax 19.8) and at the upper pole of the right kidney (SUVmax 11.0). There were no other uptake signals detected suggestive of distant metastases. Furthermore, octreotide scintigraphy showed similar mild uptake signals in the primary rectal lesion and right renal tumor (Figure 2). Taken together, the most probable diagnosis for the renal tumor was that it was a solitary metastatic lesion from the rectal NEC. Thus, the patient was diagnosed with rectal NEC cT3N0M1a, cStage IVA. Intensive systemic chemotherapy with cisplatin plus irinotecan was initiated. During the treatment, the tumor response was evaluated regularly by contrast-enhanced CT scans, and at the completion of the fourth course of chemotherapy, both the primary and metastatic tumors were evaluated radiographically to be stable diseases according to the Response Evaluation Criteria in Solid Tumors (RECIST) criteria. Since it would have been difficult to cure the intractable disease by systemic chemotherapy alone and there were no new metastatic lesions detected, we chose to perform a simultaneous radical resection of the two lesions after multidisciplinary, in-depth discussions. We proceeded with laparoscopic low anterior resection along with a diverting loop ileostomy and simultaneous partial nephrectomy. On laparoscopic examination, there were no peritoneal disseminations and the tumor at the upper pole of the right kidney was surrounded by Gerota's fascia, a finding compatible with renal metastasis, which was extirpated laparoscopically with satisfactory circumferential clearance (Figure 3).

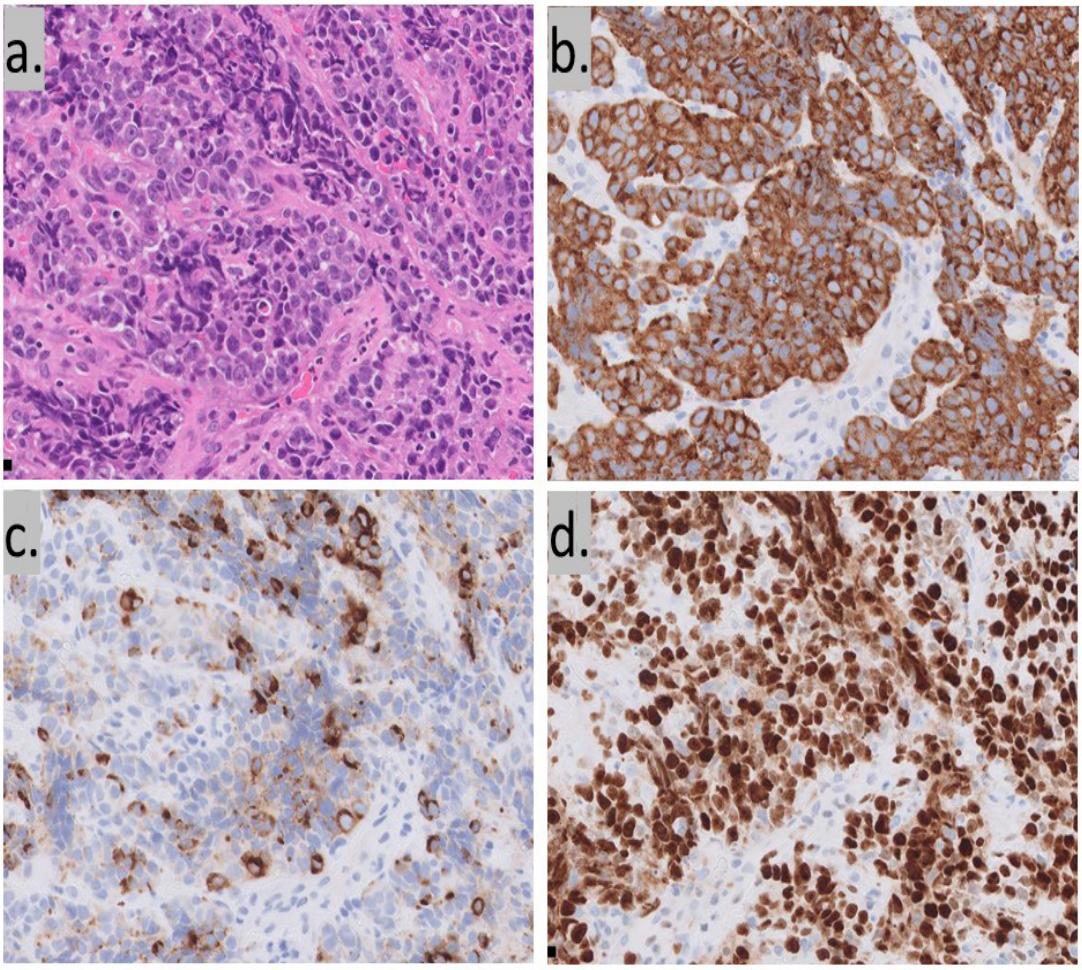

Figure 1: Microscopic findings of the biopsied specimen from the rectum. Carcinoma cells with a high N/C ratio and prominent nucleoli showed an infiltrative proliferation (hematoxylin and eosin staining) **(a)**. Immunohistochemical staining was positive for synaptophysin **(b)** and chromogranin A **(c)**, and the Ki-67 labeling index was evaluated as higher than 90% **(d)**. All the figures (**(a)- (d)**) were taken by 40x objective lens.

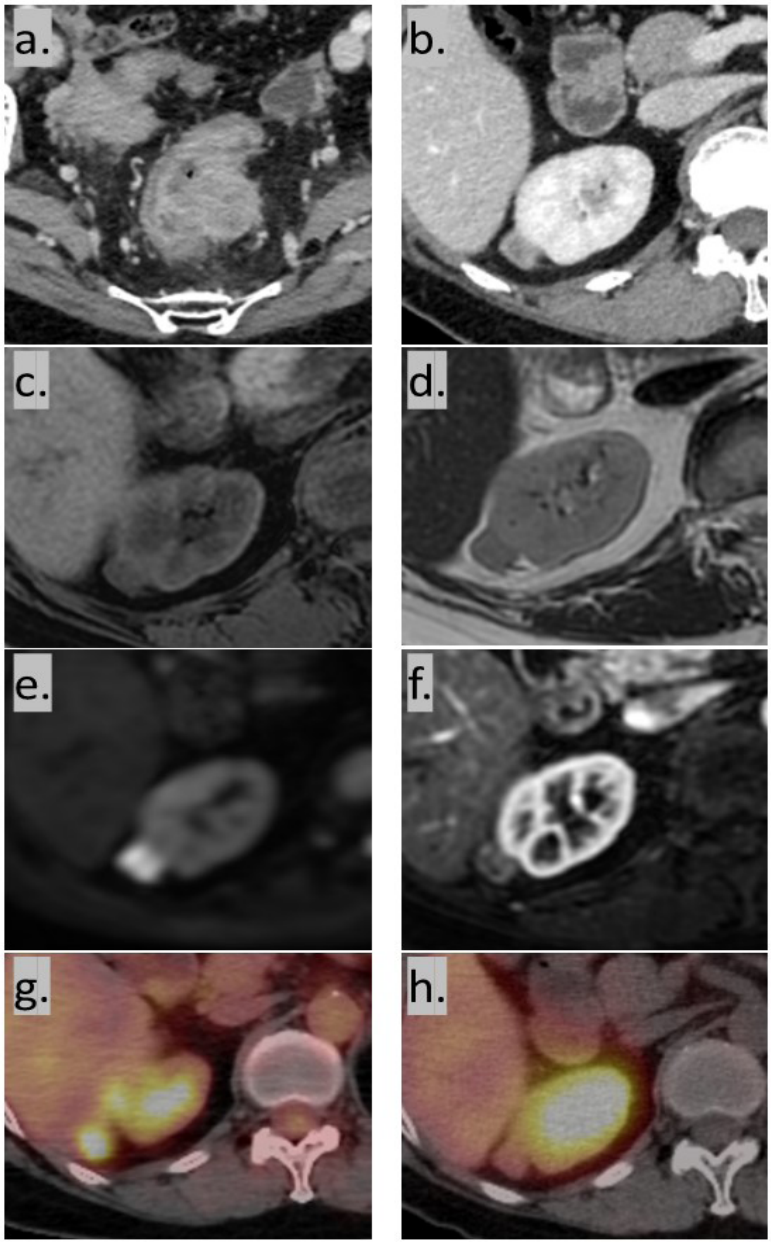

Figure 2: Preoperative imaging findings. Abdominal contrast-enhanced CT **(a, b)** showed a 30-mm tumor on the anterior-left wall of the rectum with a sign of infiltration beyond the wall **(a)**, along with an enhanced mass lesion of 15 mm in size at the upper pole of the right kidney **(b)**. On renal MR images **(c-f)**, the renal tumor was depicted as an isointense and hyperintense mass in comparison to renal parenchyma on T1- **(c)** and T2- **(d)** weighted images, respectively. Furthermore, the mass lesion showed a hyperintense signal on diffusion-weighted images **(e)** and a clear enhancement with contrast material **(f)**. FDG-PET **(g)** and octreotide scintigraphy **(h)** showed significant (SUVmax 11.0) and mild uptake in the mass lesion at the upper pole of the right kidney, respectively.

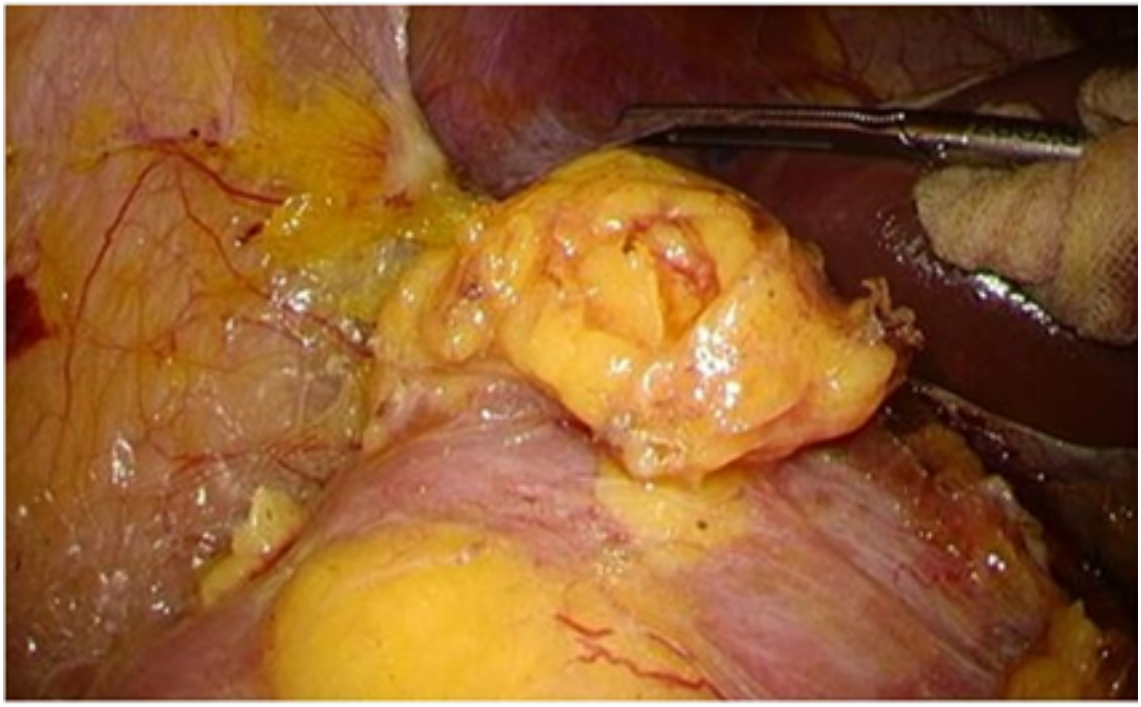

Figure 3: Surgical findings. The tumor at the upper pole of the right kidney was covered by Gerota's fascia, suggestive of a tumor arising from the kidney. There was no evidence of any metastases in the abdominal cavity.

Macroscopically, the resected specimens of the rectal and renal lesions were a T3 tumor of type 2 (55×50 mm) and a white, solid tumor (20×10 mm), respectively. As in the biopsied samples, pathological findings of the rectal tumor showed that carcinoma cells with a high N/C ratio and prominent nucleoli proliferated extensively in an infiltrative way and were immunopositive for synaptophysin and chromogranin A with a Ki-67 index of 80-90%, all of which were compatible with NEC (Figure 4). There were no components of adenocarcinoma detected and prominent lymphovascular invasion was evident. With regard to the histological assessment of response to preoperative systemic chemotherapy, the treatment effect was minimal: tumor cell necrosis or degeneration was present in less than one-third of the entire lesion. Based on the pathological similarities confirmed by the two pathologists (HK and KN), the renal tumor was diagnosed as a solitary renal metastasis from the rectal NEC (Figure 4), resulting in a final diagnosis of ypT3N0M1a, ypStage IVA. The postoperative course was uneventful and she was discharged on the 13th day after the operation. The patient is currently being monitored carefully, undergoing three-monthly CT scans without any adjuvant chemotherapy. At two years after the operation, there is no evidence of local recurrence or distant metastasis.

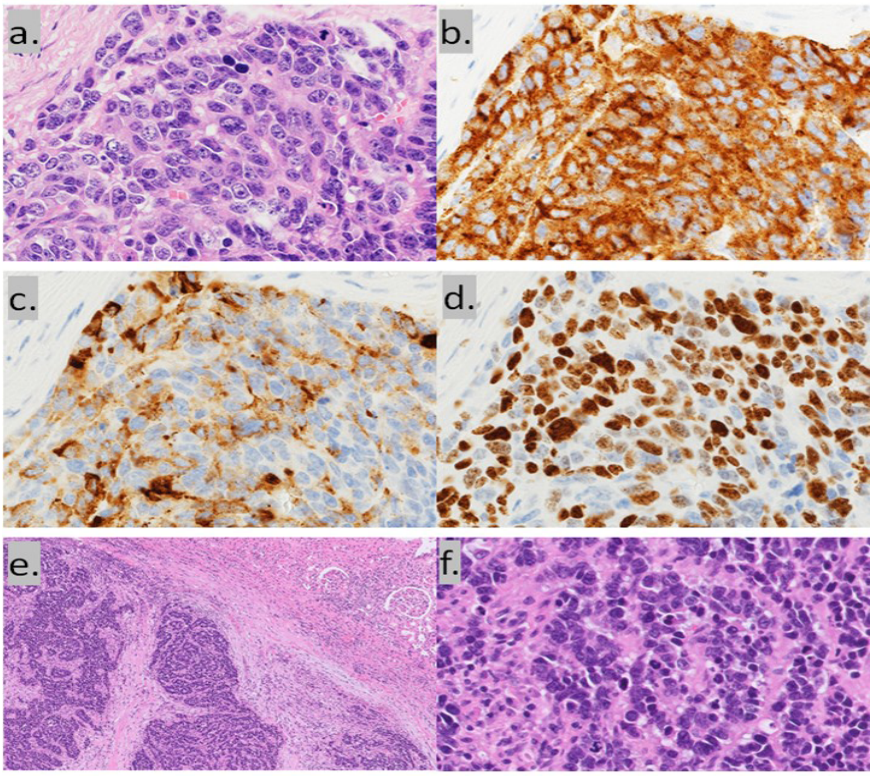

Figure 4: Microscopic findings of the resected specimen of the rectum **(a-d)** and kidney **(e,f).** In both tumors from the rectum **(a)** and kidney **(e,f),** carcinoma cells with a high N/C ratio and prominent nucleoli proliferated in an infiltrative pattern similar to that found in biopsied samples (hematoxylin and eosin staining). Immunostaining was positive for synaptophysin **(b)** and chromogranin A **(c),** and the Ki-67 labeling index was 80 to 90% **(d)** in the rectal tumor. Figures 4a-4d and 4f were taken by 40x objective lens, and figure 4e was taken by 4x objective lens.

Genetic Mutation Profiles

Whole exome and genome sequencing showed 76 and 73 biologically significant exonic mutations including amino acid substitution, frameshift and deletion except synonymous mutations in the primary tumor (1T) and the renal metastatic lesion (3KM), respectively (Figure 5). Of these mutations, 63 were common, accounting for 82.9% and 86.3% in 1T and 3KM, respectively, indicating that the primary and metastatic tumors had very similar mutation profiles. The recurrent mutations common in NEC[6] were detected in both lesions. These included two different APC mutations (p.K149Rfs*30 (frame-shift) and p.E1277X (stopgain)), a non-synonymous, pathogenic mutation in TP53 (p.C3F) and 4bp deletion in RB1 resulting in splicing alteration. There were no genetic mutations detected in KRAS or BRAF.

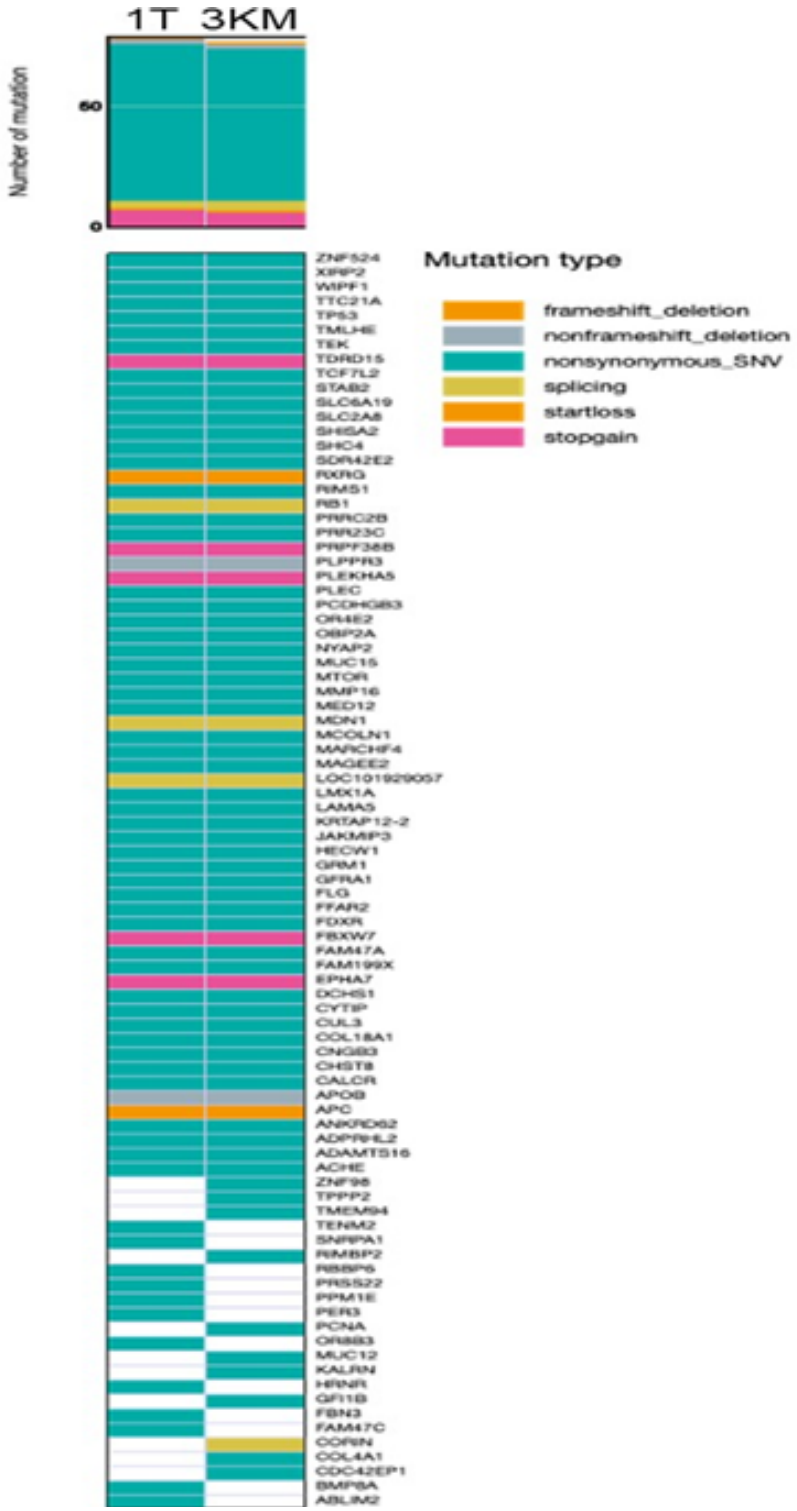

Figure 5: Genetic mutation profiles. Whole exome sequencing showed 76 and 73 somatic mutations including nonsynonymous SNV and indel mutations in the primary tumor (1T) and the renal metastatic lesion (3KM), respectively. Of these mutations, 63 were common, indicating that the primary and metastatic tumors had very similar mutation profiles.

Drug Sensitivity Screening Tests

The Patient-Derived Cell Lines (PDCs) were established from the primary and metastatic lesions, named JC-581-TR and JC-581-Ren. Using these PDCs, we examined the drug sensitivity to originally established drug inhibitor library consisting of target well-identified or approved inhibitors.[7] Neither cytotoxic inhibitors L-OHP (50 μM) nor SN-38 (500 nM) reduced cell viability, while several inhibitors (infigratinib, Bcl family inhibitors, and proteasome inhibitors) potently inhibited the growth of both JC-581-TR and JC-581-Ren cells (Figure 6). Infigratinib is an approved FGFR inhibitor for Non-Small-Cell Lung Cancer (NSCLC) and cholangiocarcinoma, but phospho-RTK (receptor tyrosine kinase) array analysis suggested that the FGFR family (FGFR1 to FGFR4) did not seem to be a direct target of infigratinib in JC-581-TR cells (Figure 7). According to a previous report,[8] infigratinib can inhibit multiple other kinases, and treatment with another FGFR inhibitor, CH5183284, did not inhibit the growth of JC-581-TR or JC-581-Ren cells at all (Figure 7). These results suggested that other targets or multiple targets of infigratinib may play an important role in JC-581-TR and JC-581-Ren cell growth. Obatoclax, a Bcl-2/Bcl-xL/Mcl-1 inhibitor, showed a marked suppression of cell viability in JC-581-TR cells. Moreover, a potent Bcl-2/Bcl-xL dual inhibitor, navitoclax, also inhibited the cell growth of JC-581-TR (Figure 7), indicating that the cell survival of JC-581-TR might be highly dependent on Bcl family proteins.

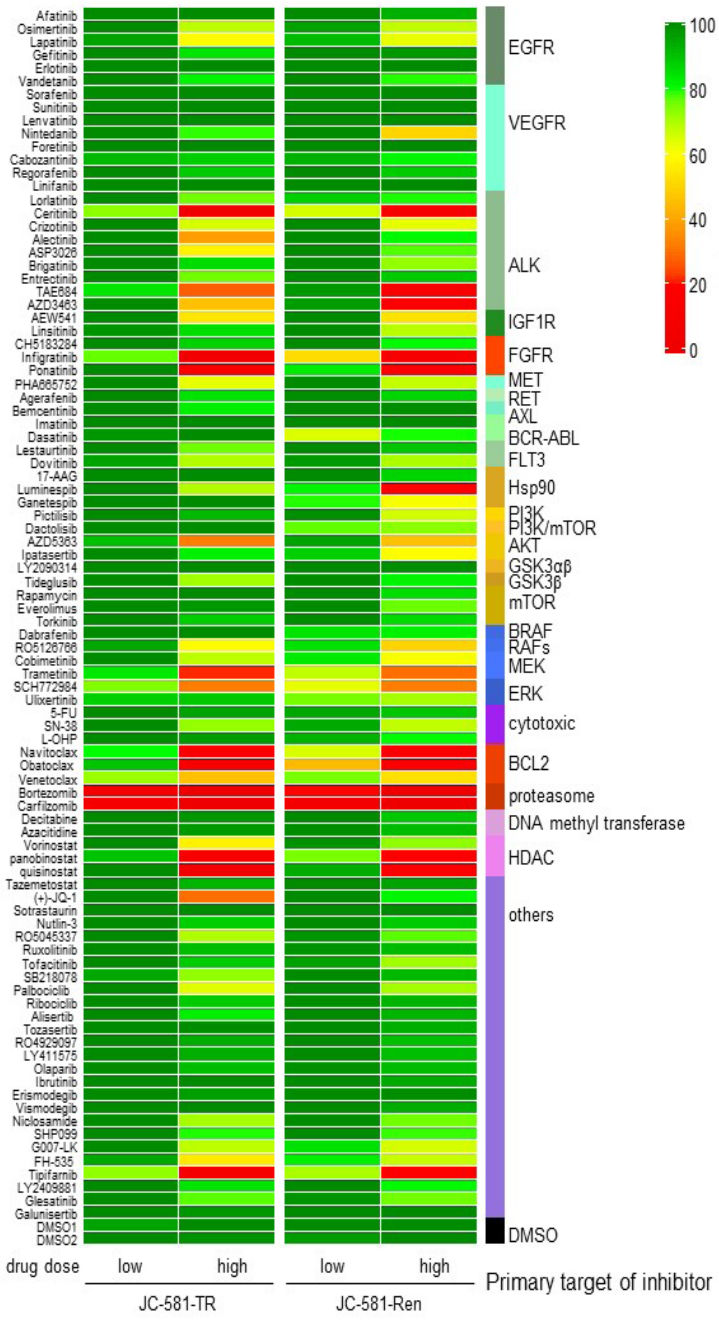

Figure 6: Drug sensitivity screening tests using PDCs established from the primary and metastatic lesions (JC-581-TR and JC-581-Ren, respectively). A heatmap shows that several inhibitors (infigratinib, Bcl family inhibitors, and proteasome inhibitors) exerted a significant growth inhibition of both JC-581-TR and JC-581-Ren cells. In contrast, neither cytotoxic inhibitors L-OHP (50 μM) nor SN-38 (500 nM) reduced cell viability.

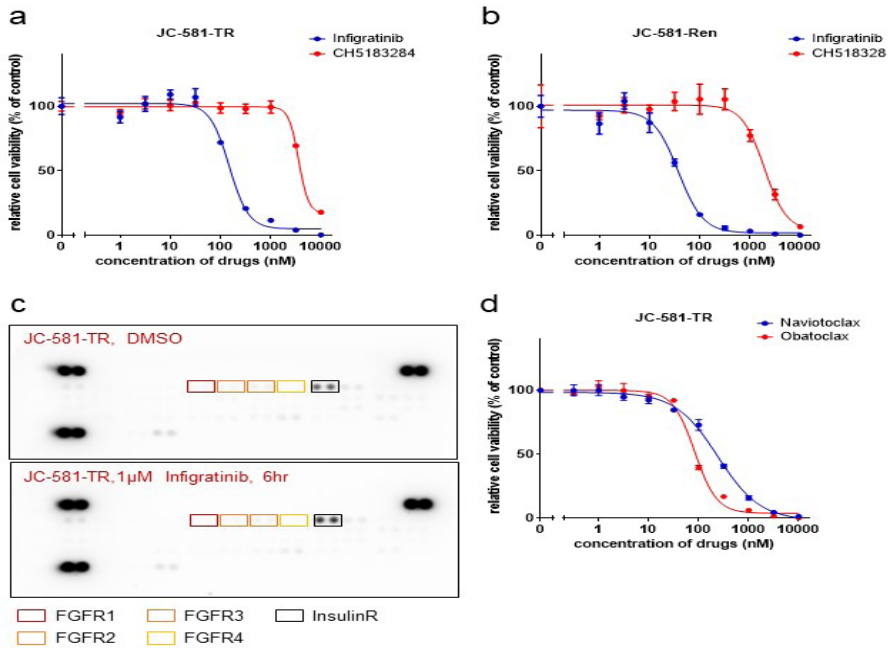

Figure 7: Drug sensitivity profiles. The growth of JC-581-TR and JC-581-Ren cells was not inhibited by administration of a different FGFR inhibitor, CH5183284 **(a,b).** Phospho-RTK array analysis shows that the FGFR family (FGFR1 to FGFR4) was unlikely to be a direct target of infigratinib in JC-581-TR cells **(c).** Obatoclax, a Bcl-2/Bcl-xL/Mcl-1 inhibitor, and navitoclax, a potent Bcl-2/Bcl-xL dual inhibitor, showed a marked suppression of cell viability in JC-581-TR cells **(d).**

Methods

The patient provided written informed consent for research use of samples including genetic analyses, establishment of PDCs and drug screening tests. Analyses were performed in accordance with protocols approved by the Institutional Review Board of the Japanese Foundation for Cancer Research.

Whole Exome and Whole Genome Sequencing

The sequence library for whole exome sequencing was prepared using a SureSelect V6 kit (Agilent Technologies). Then 151 bp paired-end libraries were subjected to mass sequencing using a HiSeq 2000 (Illumina). The sequence library for whole genome sequencing was prepared using TruSeq DNA PCR-Free (Illumina) to obtain a final library of 300-400 bp average insert size. The sequence data were processed through the Genomon pipeline (http://genomon.hgc.jp/exome/). The sequence reads were aligned to the NCBI Human Reference Genome Build 37 hg19 with BWA version 0.5.10 using default parameters (http://bio-bwa.sourceforge.net/). PCR duplicate reads were removed with Picard (http://www.picard.sourceforge.net). Mutation calling was performed using the EBcall algorithm,[9] and somatic mutations were called by comparing a tumor specimen and its matched normal colon tissue. The mutation was annotated by ANNOVAR (http://www.openbioinformatics.org/annovar/).

Establishment of patient-derived cells (PDCs) and culture condition

JC-581-TR and JC-581-Ren cells were established from surgically resected tumor samples of the primary and metastatic lesions using StemPro-hESC medium (Invitrogen) supplemented with 1.6% BSA (Invitrogen), 8 ng/ml bFGF (Nacalai Tesque), 100 μM 2-Mercapto-ethanol (Invitrogen), 10 μM Y-27632 (LC Laboratories), and 1×antibiotic–antimycotic mixed stock solution (Nacalai Tesqu). In brief, a few pieces of tumors from primary and renal metastasized site were obtained right after surgical resection. Tumor pieces were immediately placed in ice-cold culture medium with antibiotic-antimycotic (Gibco). Tumor tissues were cut into small fragments, and washed twice with ice-cold PBS supplemented with antibiotic–antimycotic. Tumor pellets were enzymatically digested with collagenase/dispase (Roche) and DNase I in StemPro-hESC medium for 30 to 60 minutes. After washing with antibiotic–antimycotic and 0.2% BSA-containing PBS, the cell pellets were cultured in the StemPro-hESC medium to establish the patient-derived JC-581-TR or JC-581-Ren cell lines. After establishing the cells, cell line authentication with 10 locus STR analysis was performed (Supplementary Table S1). The picture of the established cell line was shown in Supplementary Figure S1.

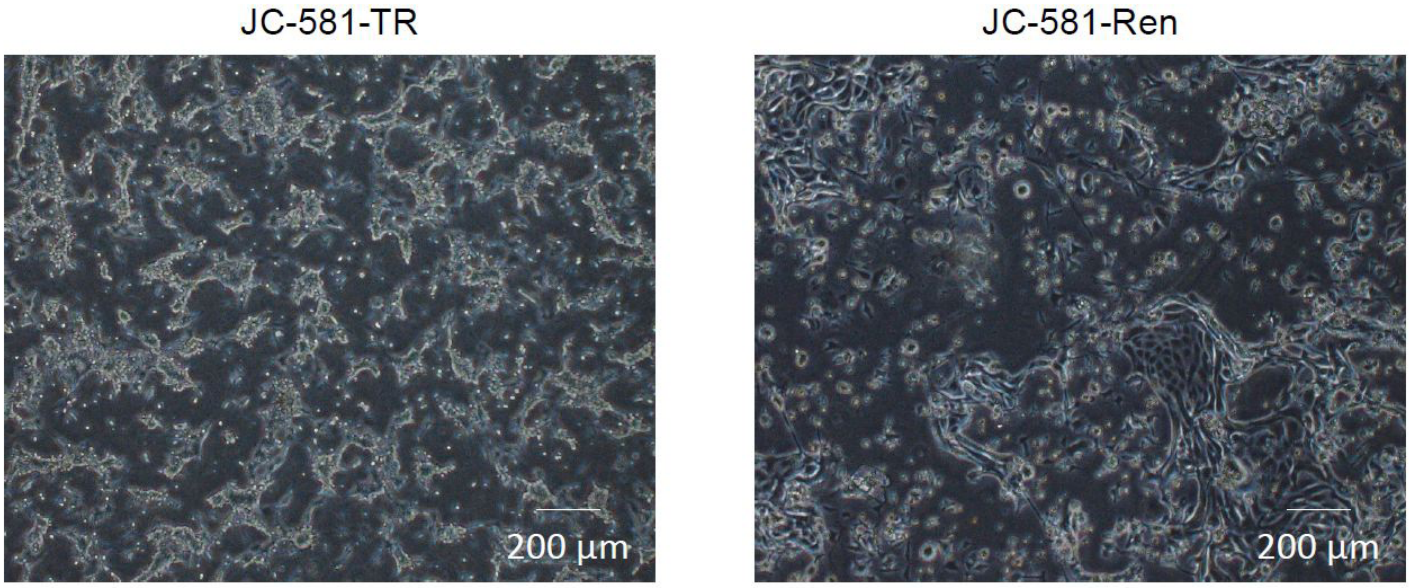

Supplementary Figure S1: Photos of the established patient derived cancer cells. JC-581-TR cells, established from primary tumor in rectum and JC-581-Ren cells from the renal metastasized tumor was cultured in the collagen coated culture dishes and taken photos with the phase contrast microscope. Scale bars are shown in the picture.

allele data										
Locus	Adjascent Normal (JC581-Normal)		Primary tumor (1T) (JC581-TR)		Renal metastatic lesion (3KM) (JC-581-Ren)		JC-581-TR_cell		JC-581-Ren_cell	
TH01	9		9		9		9		9	
D21S11	30		30		30		30		30	
D5S818	10	12	10	12	10	12	10	12	10	12
D13S317	10	12	10	12	10	12	10		10	12
D7S820	8	12	8	12	8	12	8	12	8	12
D16S539	11	12	11	12	11	12	11	12	11	12
CSF1PO	11	12	11	12	11	12	11	12	11	12
AMEL	X		X		X		X		X	
vWA	17	18	17	18	17	18	17	18	17	18
TPOX	8	11	8	11	8	11	8	11	8	11
	Complete match with other 4 samples.		Complete match with other 4 samples.		Complete match with other 4 samples.		*Evaluation value (EV) between JC581-Normal and JC581-TR_cell was 0.97, 0.97, which was high enough to consider to be identical.		Complete match with other 4 samples.	

Supplementary Table S1: The information of the STR analysis of tumor tissues and the established cells

Reagents

Infigratinib was purchased from Shanghai Biochempartner. CH5183284 was purchased from ActiveBiochem. Obatoclax and Navitoclax were purchased from AdooQ BioScience (Irvine, CA, USA). All inhibitors were dissolved in Dimethyl Sulfoxide (DMSO) for the experiments. Detailed information of the other inhibitors used for the originally established drug inhibitor library is shown in Table 1.

drug name	solvent	supplier
Ganetespib	DMSO	Adooq Bioscience
Dabrafenib	DMSO	Adooq Bioscience
BEZ235	DMSO	Adooq Bioscience
RO5126766	DMSO	Adooq Bioscience
Cobimetinib	DMSO	Adooq Bioscience
Trametinib	DMSO	Adooq Bioscience
SCH772984	DMSO	Adooq Bioscience
BVD-523	DMSO	Adooq Bioscience
GDC0068	DMSO	Adooq Bioscience
ABT263	DMSO	Adooq Bioscience
Obatoclax	DMSO	Adooq Bioscience
ABT199	DMSO	Adooq Bioscience
Decitabine	DMSO	Adooq Bioscience
Azacitidine	DMSO	Adooq Bioscience
Vorinostat	DMSO	Adooq Bioscience
Panobinostat	DMSO	Adooq Bioscience
Quisinostat	DMSO	ShangHai Biochempartner
Tazemetostat	DMSO	Adooq Bioscience
(+)-JQ-1	DMSO	ShangHai Biochempartner
Sotrastaurin	DMSO	Adooq Bioscience
Nutlin-3	DMSO	Adooq Bioscience
RO5045337	DMSO	Adooq Bioscience
Ruxolitinib	DMSO	Adooq Bioscience
Tofacitinib	DMSO	Adooq Bioscience
Palbociclib	water	Adooq Bioscience
Ribociclib	DMSO	Adooq Bioscience
Alisertib	DMSO	Adooq Bioscience
Tozasertib	DMSO	Adooq Bioscience
RO4929097	DMSO	Adooq Bioscience
LY411575	DMSO	Adooq Bioscience
LY2090314	DMSO	Adooq Bioscience
Tideglusib	DMSO	Adooq Bioscience
Olaparib	DMSO	ShangHai Biochempartner
Ibrutinib	DMSO	Adooq Bioscience
Erismodegib	DMSO	ShangHai Biochempartner
Vismodegib	DMSO	Adooq Bioscience
Bortezomib	DMSO	Adooq Bioscience
Carfilzomib	DMSO	Adooq Bioscience
Niclosamide	DMSO	ShangHai Biochempartner
OSI906	DMSO	Adooq Bioscience
5-FU	DMSO	Adooq Bioscience
SN-38	DMSO	Adooq Bioscience
SHP099	DMSO	ShangHai Biochempartner
Regorafenib	DMSO	Adooq Bioscience
G007-LK	DMSO	ShangHai Biochempartner
LY2409881	DMSO	Adooq Bioscience
Entrectinib	DMSO	Adooq Bioscience
Dovitinib	DMSO	Adooq Bioscience
MGCD-265	DMSO	Adooq Bioscience
Galunisertib	DMSO	Adooq Bioscience
Linifanib	DMSO	Adooq Bioscience
AZD3463	DMSO	BioVision
AZD5363	DMSO	Adooq Bioscience
AUY922	DMSO	ShangHai Biochempartner
R428	DMSO	ShangHai Biochempartner
RXDX105	DMSO	ShangHai Biochempartner
Crizotinib	DMSO	ShangHai Biochempartner
Ceritinib (LDK378)	DMSO	ActiveBiochem
Alectinib	DMSO	ActiveBiochem
TAE684	DMSO	ChemieTek
AP26113	EtOH	ShangHai Biochempartner
Lorlatinib (PF3922)	DMSO	ActiveBiochem
ASP3026	DMSO	ChemieTek
XL184	DMSO	ActiveBiochem
Vandetanib	DMSO	ShangHai Biochempartner
E7080	DMSO	Selleck
CEP701	DMSO	Calbiochem
Foretinib	DMSO	Adooq Bioscience
Afatinib (BIBW2992)	DMSO	ChemieTek
Erlotinib	DMSO	LC laboratories
Gefitinib	DMSO	LC laboratories
Lapatinib	DMSO	LC laboratories
Osimertinib (AZD9291)	DMSO	Selleck
PHA665752	DMSO	Tocris Bioscience
AEW541	DMSO	ActiveBiochem
Sorafenib	DMSO	Selleck
Sunitinib	DMSO	Selleck
BIBF1120	DMSO	Selleck
CH5183284	DMSO	ActiveBiochem
BGJ398	DMSO	ShangHai Biochempartner
Ponatinib	DMSO	Selleck
Imatinib	DMSO	LC laboratories
17-AAG	DMSO	LC laboratories
GDC0941	DMSO	LC laboratories
Rapamycin	DMSO	AG Scientific
Everolimus	DMSO	Chem Scene
PP242	DMSO	Adooq Bioscience
SB218078	DMSO	Tocris Bioscience
Dasatinib	DMSO	Selleck
FH-535	DMSO	Adooq Bioscience
Tipifarnib	DMSO	Adooq Bioscience
L-OHP	DMSO	wako

Table 1: The information of the inhibitors using for the originally established drug inhibitor library.

Drug screening

3,000 cells/well were seeded in triplicate in 96-Well Collagen-Coated Plates (IWAKI) and cultured for 24 hours. Cells were then treated with the originally established drug inhibitor library at a low or high concentration. After 72 hours of incubation, cell viability was assessed using CellTiter-Glo assay reagent (Promega) by measuring luminescence with a Tristar LB941 microplate luminometer (Berthold Technologies). The relative cell viability was calculated as a ratio to the DMSO control. The average relative cell viability was shown as a heat map using the ComplexHeatmap package (version 2.4.3, R version 4.0.2). Original data are shown in Table 2.

					JC-581-TR		JC-581-Ren			
Drug name		Targets	conc. (low)	conc. (high)	low	high	low	high		Relative Cell Viability
BIBW2992	Afatinib	EGFR	10 nM	100 nM	108.2	102.4	102.4	93.4		1.0
AZD9291	Osimertinib	EGFR	100 nM	1 μM	108.7	68.2	95.7	67.9		16.0
Lapatinib	Lapatinib	EGFR	200 nM	2 μM	95.9	59.1	91.6	63.2		31.0
Gefitinib	Gefitinib	EGFR	100 nM	1 μM	102.9	84.3	101.5	97.2		46.0
Erlotinib	Erlotinib	EGFR	100 nM	1 μM	126.5	120.2	115.4	114.5		61.0
Vandetanib	Vandetanib	EGFR	100 nM	1 μM	110.5	82.0	100.0	79.5		76.0
Sorafenib	Sorafenib	VEGFR2	100 nM	1 μM	120.4	105.3	115.0	105.3		91.0
Sunitinib	Sunitinib	VEGFR2	100 nM	1 μM	108.8	110.5	111.2	107.2		106.0
E7080	Lenvatinib	VEGFR2	100 nM	1 μM	127.9	113.0	104.7	99.4		121.0
BIBF1120	Nintedanib	VEGFR2	100 nM	1 μM	116.7	79.2	102.2	50.6		
Foretinib	Foretinib	VEGFR2	100 nM	1 μM	134.3	100.6	119.5	101.3		
XL184	Cabozantinib	VEGFR2	100 nM	1 μM	92.0	88.1	93.2	81.5		
Regorafenib	Regorafenib	VEGFR	100 nM	1 μM	112.9	88.4	104.9	88.4		
Linifanib	Linifanib	KDR	100 nM	1 μM	115.8	102.5	111.7	105.7		
PF3922	Lorlatinib	ALK	100 nM	1 μM	102.0	75.7	87.9	79.7		
LDK378	Ceritinib	ALK	100 nM	1 μM	73.4	2.2	65.4	9.4		
Crizotinib	Crizotinib	ALK	100 nM	1 μM	100.1	65.2	101.3	63.0		
Alectinib	Alectinib	ALK	100 nM	1 μM	135.3	38.7	113.2	81.1		
ASP3026	ASP3026	ALK	100 nM	1 μM	99.6	57.2	113.0	77.7		
AP26113	Brigatinib	ALK	100 nM	1 μM	106.4	85.8	108.8	72.7		
entrectinib	Entrectinib	ALK	100 nM	1 μM	107.5	75.7	100.5	88.8		
TAE684	TAE684	ALK	100 nM	1 μM	84.5	27.5	97.6	12.8		
AZD3463	AZD3463	ALK	100 nM	1 μM	103.3	46.0	97.0	15.3		
AEW541	AEW541	IGF1R	100 nM	1 μM	116.8	54.3	106.8	53.7		
OSI906	Linsitinib	IGF1R	100 nM	1 μM	98.2	85.5	102.5	68.7		
CHIR83284	CHIR83284	FGFR	100 nM	1 μM	111.5	87.5	107.2	80.8		
BGJ398	Infigratinib	FGFR	100 nM	1 μM	76.5	3.1	52.3	11.8		
Ponatinib	Ponatinib	FGFR	100 nM	1 μM	111.2	14.4	83.1	14.9		
PHA665752	PHA665752	MET	100 nM	1 μM	120.5	63.0	110.4	67.6		
RXDX105	Agerafenib	RET	100 nM	1 μM	102.8	84.3	99.2	86.7		
R428	Bemcentinib	Axl	100 nM	1 μM	105.1	82.8	114.8	99.5		
Imatinib	Imatinib	bcr-abl	100 nM	1 μM	115.0	106.1	109.3	108.8		
Dasatinib	Dasatinib	bcr-abl	100 nM	1 μM	97.9	109.6	64.6	79.8		
CEP701	Lestaurtinib	FLT3	100 nM	1 μM	113.2	75.8	120.1	89.6		
Dovitinib	Dovitinib	FLT3	100 nM	1 μM	95.5	69.7	97.5	70.3		
17-AAG	17-AAG	HSP90	10 nM	100 nM	118.9	100.3	103.3	87.1		
AUY922	Luminespib	HSP90	10 nM	100 nM	112.4	69.4	81.6	19.5		
Ganetespib	Ganetespib	HSP90	10 nM	100 nM	104.3	100.4	79.5	61.0		
GDC0941	Pictilisib	PI3K	100 nM	1 μM	113.6	91.7	99.2	65.9		
BEZ235	Dactolisib	PI3K/mTOR	100 nM	1 μM	102.4	99.6	76.8	73.6		
AZD5363	AZD5363	AKT	100 nM	1 μM	90.6	32.5	95.5	46.4		
GDC0068	Ipatasertib	AKT	100 nM	1 μM	109.1	82.4	87.9	59.8		
LY2090314	LY2090314	GSK3a/b	100 nM	1 μM	137.6	114.6	138.8	99.2		
Tideglusib	Tideglusib	GSK3b	100 nM	1 μM	104.3	71.4	99.5	82.0		
Rapamycin	Rapamycin	mTOR	100 nM	1 μM	117.8	107.1	108.4	85.4		
Everolimus	Everolimus	mTOR	100 nM	1 μM	124.7	97.7	108.1	76.2		
PP242	Torkinib	mTOR	100 nM	1 μM	115.0	88.1	121.3	86.2		
Dabrafenib	Dabrafenib	BRAF	100 nM	1 μM	100.7	100.2	84.4	82.3		
RO5126766	RO5126766	RAF	100 nM	1 μM	94.6	59.1	84.8	50.3		
Cobimetinib	Cobimetinib	MEK	10 nM	100 nM	103.2	68.2	83.7	60.9		
Trametinib	Trametinib	MEK	10 nM	100 nM	83.8	21.5	67.8	30.0		
SCH772984	SCH772984	ERK	100 nM	1 μM	74.4	32.7	63.2	32.5		
BVD-523	Ulixertinib	ERK	100 nM	1 μM	87.9	89.1	75.2	70.9		
5-FU	5-FU	DNA/RNA synthesis	10 μM	100 μM	116.3	95.4	94.8	89.6		
SN-38	SN-38	TOPO1	50 nM	500 nM	102.3	72.6	94.7	67.8		
L-OHP	L-OHP	DNA synthesis	5 μM	50 μM	103.4	97.0	92.9	80.4		
ABT263	Navitoclax	Bcl-X/L,Bcl-2	100 nM	1 μM	80.4	14.2	65.1	14.4		
Obatoclax	Obatoclax	Bcl-X/L,Bcl-2,Mcl-1	100 nM	1 μM	89.8	11.7	44.8	15.2		
ABT199	Venetoclax	Bcl-X/L,Bcl-2	100 nM	1 μM	72.0	46.1	75.1	53.1		
Bortezomib	Bortezomib	proteasome	10 nM	100 nM	7.8	1.2	20.1	2.2		
Carfilzomib	Carfilzomib	proteasome	10 nM	100 nM	9.5	1.7	7.2	1.0		
Decitabine	Decitabine	Methyl	100 nM	1 μM	107.4	97.8	102.6	89.1		
Azacitidine	Azacitidine	Methyl	100 nM	1 μM	107.7	97.2	99.5	91.4		
Vorinostat	Vorinostat	HDAC	100 nM	1 μM	115.8	57.1	98.8	72.9		
panobinostat	panobinostat	HDAC	10 nM	100 nM	90.0	9.9	75.0	18.0		
quisinostat	quisinostat	HDAC	10 nM	100 nM	127.0	4.1	94.0	13.9		
Tazemetostat	Tazemetostat	EZH2	100 nM	1 μM	125.9	92.3	112.6	95.5		
(+)-JQ-1	(+)-JQ-1	BET	100 nM	1 μM	116.0	30.0	115.4	81.5		
Sotrastaurin	Sotrastaurin	panPKC	100 nM	1 μM	126.6	119.9	115.9	113.7		
Nutlin-3	Nutlin-3	MDM2	100 nM	1 μM	122.2	88.1	101.8	88.7		
RO5045337	RO5045337	MDM2	100 nM	1 μM	107.8	69.8	98.0	77.3		
Ruxolitinib	Ruxolitinib	JAK	100 nM	1 μM	114.4	91.1	98.5	91.6		
Tofacitinib	Tofacitinib	JAK	100 nM	1 μM	101.9	88.4	95.8	71.5		
SB218078	SB218078	CHK1	100 nM	1 μM	94.7	72.9	106.7	92.0		
Palbociclib	Palbociclib	CDK4/6	100 nM	1 μM	107.3	64.0	105.4	70.8		
Ribociclib	Ribociclib	CDK4/6	100 nM	1 μM	112.6	88.7	99.7	92.6		
Alisertib	Alisertib	aurorsA	100 nM	1 μM	109.3	82.3	101.1	92.5		
Tozasertib	Tozasertib	panaurora	100 nM	1 μM	123.0	99.6	113.5	93.7		
RO4929097	RO4929097	γsecretase	100 nM	1 μM	116.2	93.7	113.2	90.6		
LY411575	LY411575	γsecretase	100 nM	1 μM	118.2	93.7	105.0	90.9		
Olaparib	Olaparib	PARP	100 nM	1 μM	114.3	91.1	99.1	91.4		
Ibrutinib	Ibrutinib	Btk	100 nM	1 μM	115.4	130.5	111.5	94.3		
Erismodegib	Erismodegib	smo	100 nM	1 μM	121.4	96.3	107.8	99.5		
Vismodegib	Vismodegib	smo	100 nM	1 μM	116.7	101.5	115.1	93.8		
Niclosamide	Niclosamide	STAT3	100 nM	1 μM	103.9	70.8	103.7	75.6		
SHP099	SHP099	SHP2	500 nM	5 μM	113.2	79.6	108.5	79.0		
G007-LK	G007-LK	tankyrase	200 nM	2 μM	107.2	68.5	85.0	65.4		
FH 535	FH 535	Wnt/TCF	1.5 μM	15 μM	94.8	55.4	82.5	67.4		
Tipifarnib	Tipifarnib	FPTase	1.5 μM	15 μM	72.9	6.8	70.5	15.9		
LY2409881	LY2409881	IKK	100 nM	1 μM	120.3	84.1	102.7	80.8		
MGCD-265	Glesatinib	Tie2	100 nM	1 μM	119.2	77.4	98.3	75.7		
Galunisertib	Galunisertib	TGFβ	100 nM	1 μM	113.8	97.7	108.8	102.6		
DMSO1	DMSO1				95.9	101.4	103.0	99.9		
DMSO2	DMSO2				104.1	98.6	97.0	100.1		

Table 2: Drug sensitivity of JC-581-TR and Ren.

Cell viability assay

For evaluating cell viability to each inhibitor, cells were seeded in triplicate at 3,000 cells/well in 96-well collagen-coated plates. After culture for 24 hours, the cells were treated with the indicated concentration of drugs for 72 hours. The cell viability was measured using CellTiter-Glo assay reagent as indicated in the previous section. GraphPad Prism version 9.1.2 (GraphPad Software) was used to analyze the data.

Phospho-RTK array assay

Cells were seeded at 3×10^6 cells in a collagen-coated dish and cultured for 24 hours. The cells were treated with DMSO control or 1 μM of infigratinib. After 6 hours of drug treatment, the cell lysates were collected and applied to a phospho-RTK array assay according to the manufacturer's instructions for the Proteome Profiler Human Phospho-Kinase Array Kit (R&D Systems). The signal was detected using an Amersham ImageQuant 800 (GE Healthcare).

Discussion

As metastatic malignancies in the kidney are rare and asymptomatic in most cases, their exact incidences are difficult to evaluate. In autopsy-based analysis, metastatic renal tumors were incidentally found in 7.2 to 18.8%, of which 2.9 to 4.4% were metastatic lesions derived from primary colon malignancies. [10,11] Although there are some case reports describing renal metastasis from colorectal cancers, these patients had overt multiple organ metastases besides renal tumors, [12-15] so a solitary renal metastasis from colorectal cancers is thought to be quite rare. Among published reports of colorectal NENs, only one patient with rectal NET G1 has been demonstrated to develop renal metastasis. [14] As far as we know, there have been no previous reports on a solitary metastasis from rectal NEC to the kidney.

In a retrospective study involving 100 patients with high-grade neuroendocrine colorectal carcinomas, 60% had a primary tumor located from the sigmoid colon to rectum, and 64% had already developed distant metastases at the time of the first consultation. The median Overall Survival (OS) was 14.7 months, and the 2- and 5-year OS rates were 23% and 8%, respectively, indicating a very poor prognosis. [16] According to the National Comprehensive Cancer Network (NCCN) Guidelines 2020, because of the severity of biological malignancy, multidisciplinary treatment is recommended even for resectable NEC primary lesions, and chemotherapy-based treatment such as irinotecan/cisplatin or carboplatin/etoposide is indicated for locally advanced tumors or distant metastases. [17,18] With intensive treatment, however, the Overall Response Rate (ORR) was estimated to be 42% at most [16].

In our case, four courses of systemic intensive chemotherapy with irinotecan/cisplatin were administered, resulting in the best response of Stable Disease (SD). In a multidisciplinary team meeting, we discussed the pros and cons of the continuation of systemic chemotherapy or possible radical resection of the target lesions. Considering that there are no second-line regimens established for rectal NECs and that no new metastatic lesions had appeared at the completion of four courses of chemotherapy, we concluded that radical resection of the primary and metastatic tumors could cure the disease. Furthermore, minimally invasive surgery for simultaneous resection of the two lesions was considered to be feasible by laparoscopic low anterior resection and by laparoscopic partial resection of the kidney as demonstrated by a previous report. [19] Thus, we chose to perform the laparoscopic radical resection of the target lesions.

In terms of radical resection for NECs with distant metastases, a satisfactory OS rate was achieved by upfront surgical resection of pancreatic NEC along with simultaneous liver metastases in some cases. [20] Furthermore, in 32 NEC cases of the pancreas (14), CRC (12) and others (6), liver metastases were well controlled by RFA (radiofrequency ablation) or surgery, resulting in a satisfactory OS rate. [21] Although these findings that surgical resection might yield a better OS in even some Stage IV NEC cases are encouraging, there are two limitations to be considered. As these reports were based on the previous definitions of NET rather than the new, global classification of WHO 2019, NET G3 and NEC were treated as the same disease entity. The other is that the number of cases involved is very small with various patterns of primary and metastatic sites. Although intensive systemic chemotherapy is primarily recommended for primary NECs with multi-organ metastases or recurrent NECs, there is a possibility that the prognosis can be improved by interposing radical surgical resection during systemic chemotherapy. The true benefit of surgical intervention for an improved prognosis remains to be determined through an accumulation of colorectal NEC cases according to the new version of WHO classification.

Regarding genomic in-depth analysis, genetic mutations in TP53 and RB1 are considered to be characteristic of NEC, and TP53 p.C3F is already registered as a pathogenic mutation. Although a pathogenic effect of 4bp deletion in RB1 is undetermined, this mutation is probably pathogenic, as the deleted nucleotides contained a splicing acceptor site (GTGA), thereby leading to truncation by frame shift. Consistent with this notion, it is not registered in the Human Genetic Variation Database (HGVD) (https://www.hgvd.genome.med.kyoto-u.ac.jp/), a reference database of genetic variations in the Japanese population. These observations may indicate that the RB1 mutation found in this patient is a novel pathogenic mutation.

According to our drug sensitivity screening tests, Bcl family inhibitors and proteasome inhibitors besides infigratinib can also

be effective in the treatment of NECs. Previous reports showed that NECs arising in different organs including small-cell lung cancer (SCLC) and Small-Cell Neuroendocrine Prostate Cancer (SCNPC) were sensitive to Bcl-2 inhibition. [22,23] In addition, given that Bcl-2 expression was found to be high in 64% of 25 colorectal NECs, [24] inhibitors to the Bcl family including Bcl-2 might be a therapeutic option for colorectal NECs. In a previous phase II study of a proteasome inhibitor, bortezomib, for metastatic NETs, [25] single-agent bortezomib did not induce any objective responses in the 16 enrolled, chemotherapy-naive patients. However, there is an encouraging recent article describing the possible effectiveness of inhibitors of NAE (NEDD8 (neural precursor cell expressed, developmentally downregulated 8) activating enzyme) in patients with small intestinal NETs (SI-NETs), which can exert a therapeutic effect through cell cycle regulation by inhibiting the ubiquitin-proteasome pathways resulting in p27 stabilization. [26] Considering that NAE inhibitors have been approved by the FDA (Food and Drug Administration) as therapeutic agents for high-risk MDS (myelodysplastic syndrome), and a clinical trial designed to investigate the efficacy of NAE inhibitors for AML (acute myeloid leukemia) and NSCLC patients is currently ongoing, NAE could be a promising candidate for molecular targeted therapy in colorectal NEC patients. Our comprehensive drug screening system using PDCs can serve as a platform for assessing novel therapeutics with the potential to be translated into clinical practice.

Conclusions

We performed laparoscopic radical resection for rectal NEC and its solitary renal metastasis. Since the long-term prognosis of curative resection for stage IV rectal NEC is still undetermined, post-operative careful monitoring of the patient is required. According to the findings of a comprehensive drug-sensitivity screening test, infigratinib, obatoclax and navitoclax were shown to be effective to the cancer cells established from the resected tumor samples.

References

1. Nagtegaal ID, Odze RD, Klimstra D, Paradis V, Rugge M, et al. (2020) The 2019 WHO classification of tumours of the digestive system. Histopathology 76: 182-188.
2. Kawasaki K, Rekhtman N, Quintanal-Villalonga A (2023) Neuroendocrine neoplasms of the lung and gastrointestinal system: convergent biology and a path to better therapies. Nat Rev Clin Oncol 20: 16-32.
3. Mafficini A, Scarpa A (2019) Genetics and epigenetics of gastroentero-pancreatic neuroendocrine neoplasms. Endocr Rev 40: 506-536.
4. Kawasaki K, Toshimitsu K, Matano M (2020) An Organoid biobank of neuroendocrine neoplasms enables genotype-phenotype mapping. Cell 183: 1420-1435.
5. Rinke A, Auernhammer CJ, Bodei L (2021) Treatment of advanced gastroentero-pancreatic neuroendocrine neoplasia, are we on the way to personalised medicine? Gut 70: 1768-1781.
6. Woischke C, Schaaf CW, Yang HM (2017) In-depth mutational analyses of colorectal neuroendocrine carcinomas with adenoma or adenocarcinoma components. Mod Pathol 30: 95-103.
7. Shimizu Y, Okada K, Adachi J (2022) GSK3 inhibition circumvents and overcomes acquired lorlatinib resistance in ALK-rearranged non-small-cell lung cancer. NPJ Precis Oncol 6: 16.
8. Gudernova I, Vesela I, Balek L (2016) Multikinase activity of Fibroblast Growth Factor Receptor (FGFR) inhibitors SU5402, PD173074, AZD1480, AZD4547 and BGJ398 compromises the use of small chemicals targeting FGFR catalytic activity for therapy of short-stature syndromes. Hum Mol Genet 25: 9-23.
9. Shiraishi Y, Sato Y, Chiba K (2013) An empirical Bayesian framework for somatic mutation detection from cancer genome sequencing data. Nucleic Acids Res 41: e89.
10. Wagle DG, Moore RH, Murphy GP (1975) Secondary carcinomas of the kidney. J Urol 114: 30-32.
11. Bracken RB, Chica G, Johnson DE (1979) Secondary renal neoplasms: an autopsy study. South Med J 72: 806-807.
12. Julianov A, Stoyanov H, Karashmalakov A (2004) Late renal metastasis from sigmoid adenocarcinoma. Lancet Oncol 5: 726.
13. Maruyama T, Ueda Y, Suzuki T (2013) Renal metastasis originating from colon cancer: a case report. Hinyokika Kiyo 59: 569-572.
14. Kato Y, Nakamura K, Yamada Y (2010) A rare case of metastatic renal carcinoid. BMC Urol 10: 22.
15. Waleczek H, Wente MN, Kozianka J (2005) Complex pattern of colon cancer recurrence including a kidney metastasis: a case report. World J Gastroenterol 11: 5571-5572.
16. Conte B, George B, Overman M (2016) High-grade neuroendocrine colorectal carcinomas: A retrospective study of 100 patients. Clin Colorectal Cancer 15: e1-e7.
17. Iwasa S, Morizane C, Okusaka T (2010) Cisplatin and etoposide as first-line chemotherapy for poorly differentiated neuroendocrine carcinoma of the hepatobiliary tract and pancreas. Jpn J Clin Oncol 40: 313-318.
18. Frizziero M, Spada F, Lamarca A (2019) Carboplatin in combination with oral or intravenous etoposide for extra-pulmonary, poorly-differentiated neuroendocrine carcinomas. Neuroendocrinology 109: 100-112.
19. Ng SS, Lee JF, Yiu RY (2007) Synchronous laparoscopic resection of colorectal and renal/adrenal neoplasms. Surg Laparosc Endosc Percutan Tech 17: 283-286.
20. Haugvik SP, Janson ET, Osterlund P (2016) Surgical treatment as a principle for patients with high-grade pancreatic neuroendocrine carcinoma: A Nordic multicenter comparative study. Ann Surg Oncol 23: 1721-1728.
21. Galleberg RB, Knigge U, Tiensuu Janson E (2017) Results after surgical treatment of liver metastases in patients with high-grade gastroenteropancreatic neuroendocrine carcinomas. Eur J Surg Oncol 43: 1682-1689.
22. Lochmann TL, Floros KV, Naseri M (2018) Venetoclax is effective in small-cell lung cancers with high BCL-2 expression. Clin Cancer Res 24: 360-369.
23. Corella AN, Cabiliza Ordonio MVA, Coleman I (2020) Identification of therapeutic vulnerabilities in small-cell neuroendocrine prostate cancer. Clin Cancer Res 26: 1667-1677.

24. Takizawa N, Ohishi Y, Hirahashi M (2015) Molecular characteristics of colorectal neuroendocrine carcinoma; similarities with adenocarcinoma rather than neuroendocrine tumor. Hum Pathol 46: 1890-1900.

25. Shah MH, Young D, Kindler HL (2004) Phase II study of the proteasome inhibitor bortezomib (PS-341) in patients with metastatic neuroendocrine tumors. Clin Cancer Res 10: 6111-6118.

26. Fotouhi O, Kjellin H, Juhlin CC (2019) Proteomics identifies neddylation as a potential therapy target in small intestinal neuroendocrine tumors. Oncogene 38: 6881-6897.